Talanta 189 (2018) 502–508

Contents lists available at ScienceDirect

Talanta

journal homepage: www.elsevier.com/locate/talanta

Anion-exchange polymer filament coating for ultra-trace isotopic analysis of plutonium by thermal ionization mass spectrometry

Joseph M. Mannion[a,*], Charles R. Shick Jr[b], Glenn A. Fugate[b,1], Brian A. Powell[c], Scott M. Husson[a]

[a] Department of Chemical and Biomolecular Engineering, Clemson University, 127 Earle Hall, Clemson, SC 29634, USA
[b] Savannah River National Laboratory, National Security Directorate, Aiken, SC 29808, USA
[c] Department of Environmental Engineering and Earth Sciences, Clemson University, 342 Computer Court, Anderson, SC 29625, USA

ARTICLE INFO

Keywords:
Actinide isotope ratio measurements
Environmental monitoring
Nonproliferation
Nuclear forensics
Ultra-trace analysis

ABSTRACT

A new sample loading procedure was developed for isotope measurements of ultra-trace amounts of Pu with thermal ionization mass spectrometry (TIMS) that is based on a polymer thin film architecture. The goals were to simplify single filament TIMS sample preparation for Pu, while preserving the sensitivity and accuracy of the resin bead loading method, and to eliminate sample losses experienced with the bead loading method. Rhenium filaments were degassed, dip-coated with a thin (~120 nm) hydrophobic base layer of poly(vinylbenzyl chloride) (PVBC), and spotted with an aqueous solution comprising triethylamine-quaternized PVBC and diazabicyclo[2.2.2]octane crosslinker. This procedure formed a toroidal, hydrophilic anion-exchange polymer spot surrounded by the hydrophobic base polymer. The thin film-coated filaments were direct loaded with 10 pg of New Brunswick Laboratory certified reference material (NBL CRM) 128 from a 9 M HCl matrix. Aqueous sample droplets adhered to the anion-exchange polymer spot, facilitating sample loading. Toroidal spots with a thickness of 20–30 μm generated the highest sample utilization, surpassing the sample utilization of the standard bead loading method by 175%. Measured isotopic ratios were in good agreement with the certified value of the $^{239}Pu/^{242}Pu$ ratio for NBL CRM 128. The use of dimpled filaments further aided sample loading by providing a well-shaped substrate to deposit the sample droplet. No sample losses were experienced with the thin film loading method over 65 sample analyses. Finally, polymer coatings suppressed filament aging under atmospheric conditions, enabling the bulk production of filaments with adequate shelf life for future analyses.

1. Introduction

Thermal ionization mass spectrometry (TIMS) with isotope dilution is recognized internationally as the gold standard for obtaining isotopic ratios and mass amounts of Pu [1]. Isotopic analysis of ultra-trace quantities of Pu is possible by TIMS [2,3], a technique that remains important in the fields of nuclear safeguards [4], nuclear forensics [5], and environmental monitoring [6]. While expensive and time consuming, TIMS is used for analyses requiring high levels of sensitivity and accuracy [7]. Sample loading techniques have a large influence on Pu detection limits by TIMS (direct loading ≈ 10^{11} atoms; electroplating ≈ 10^{10} atoms; resin bead loading on Re filament ≈ 10^{7} atoms; resin bead loading in Re cavity ≈ 10^{4}) [8,9] and, in some cases, contribute significantly to the time investment associated with these analyses [10].

Carbon-based filament additives have been used in sample preparation schemes for the thermal ionization of actinides since at least the 1960s, when carbon addition was identified as a means to suppress sample oxidation in early vacuum systems [11]. Decades of research has resulted in a variety of carbon incorporation methods, and carbonaceous additives are understood (or believed) to provide at least three additional benefits to sample utilization (defined as the quotient of sample atoms detected and sample atoms loaded):

1) Carbonaceous additives promote the formation of Pu-carbides [12]. The conversion of Pu to the carbide form is believed to stabilize the sample against thermal ionization, resulting in ionization at elevated temperatures [13]. As described by the Saha-Langmuir equation (Eq. (1)) [14], when the difference between the work function of a surface and the ionization energy of the deposited

* Correspondence to: Savannah River National Laboratory, National Security Directorate, Building 703-43A Room 18-7, Aiken, SC 29808, USA.
E-mail address: joseph.mannion@srs.gov (J.M. Mannion).
[1] Present Address: Oak Ridge National Laboratory, Nuclear Security & Isotope Technology Division, Oak Ridge, TN 37831, USA.

https://doi.org/10.1016/j.talanta.2018.07.048
Received 30 April 2018; Received in revised form 12 July 2018; Accepted 13 July 2018
0039-9140/

sample is negative (rhenium work function ≈ 4.7 eV [15]; Pu first ionization energy = 6.06 eV [16]), thermal ionization efficiency is positively related to the temperature of ionization. Therefore, ion production occurring at elevated temperatures vis-à-vis Pu carbide formation results in increased ionization efficiency.

$$\frac{n_+}{n_0} = \frac{g_+}{g_0} e^{\frac{W-I}{kT}} \quad (1)$$

n_+/n_0 is ionization efficiency, g_+/g_0 is the ratio of statistical weights of the ionic and atomic states, W is the work function of the ionization surface, I is the ionization energy of the sample, T is the temperature of ionization, and k is the Boltzmann constant.

2) "Carburization" or "carbonation" of rhenium filaments provides a more favorable surface for sample ionization to occur [17]. In thermal ionization processes, the work function of an ionization surface is related to ionization efficiency exponentially (Eq. (1)). Therefore, high work function materials are desired in the construction of TIMS ionization filaments (for the production of positive ions). Rhenium is a preferred filament material for TIMS analyses of Pu, in part due to its high work function [18], which can be increased further through carbon dissolution at high temperatures (> 1500 °C) [19]. Modern carburization processes often involve exposing rhenium filaments to volatile organic compounds under vacuum while resistively heating the filaments [17,20]. This process is estimated to increase the average work function of polycrystalline rhenium by ~0.4 eV [21]. Localized filament carburization also may occur with methods such as "bead loading", where small (40–300 μm) polymer beads are affixed directly upon rhenium ionization filaments [22]. Other carbonaceous additives, such as collodion, aquadag, and graphite, which are applied directly to the filament before analysis, have been tested for use in Pu analysis by TIMS [17] and contribute to filament carburization when heated [23].
3) Extractive polymeric materials, such as anion-exchange resin beads, are capable of concentrating the sample into a geometrically small region on the ionization surface, producing a narrower ion beam [22]. This aides in ion-beam focusing, resulting in increased ion transmission into the mass spectrometer [7]. Bead loading, involving concentration of Pu on resin beads [24], has shown improved sample utilization compared to more dispersed means of sample loading, such as electrodeposition and simple direct loading [8]. Anion-exchange resins often are used in the cases of Pu sample loading, as Pu readily forms an anionic complex in concentrated nitric [25] and hydrochloric acid [26].

Ion source geometries other than flat ribbon filaments have been studied in efforts to increase ionization efficiency and focus ions emitted from the ion source. Modified filament designs have aimed to increase contact, or the number of interactions, between the sample atoms and the ionization surface. In TIMS analysis of Pu, the majority of the loaded sample is emitted from the filament as neutral gas atoms (ionization efficiency: direct loading ≈ 0.01–0.1%; resin bead loading ≈ 0.1 – 1.0%) [9]. By loading the sample in a concave ionization source, neutral gas atoms emitted from the initial point of loading have opportunities to interact with the ionization surface multiple times. In one design, the cavity source, high ionization efficiencies (~10%) relative to other methods were achieved by loading the Pu sample into the back of a capped rhenium tube heated by an electron gun [27]. It is theorized that neutral gas atoms produced at the closed end of the tube will scatter along the inside of the tube, thus having multiple opportunities to collide with the tube surface and become ionized. Porous ion emitter designs have emulated this concept by creating micro-porous rhenium structures on electrically heated filaments [7]. Other ion source geometries include the "boat" or V-shaped filament, where rhenium ribbon is crimped into a trough shape. V-shaped filaments have been shown to increase ion focusing [28] and aid in sample loading [17].

Aggarwal et al. recently reported a membrane-based method of sample loading utilizing phosphate-bearing extractant polymers [29]. Two methods of membrane loading are reported by Aggarwal et al.: 1) membrane sections were submerged in sample bearing solution before washing and being placed onto filaments; and 2) membrane sections were loaded in solution, washed, then held in contact with the filament by hand while slowly heating the filament, melting and depositing the sample bearing polymer onto the filament. Although novel, these loading methods result in a more dispersed ion production region than in the case of bead loading. Additionally, membrane sections must be manipulated by hand after exposure to radioisotopes, a challenge shared with the bead loading method.

The goals for this work were to simplify sample loading for TIMS analysis of Pu while retaining the sensitivity afforded by the established bead loading method, and to eliminate sample losses often experienced with the bead loading method (up to 25% in some cases [7]). The objective was to develop a Pu extractive filament pre-coating that retains the ion focusing afforded by the resin bead method while also making direct loading by pipette possible, thereby eliminating the need to handle and position radioisotope-bearing anion-exchange material. This objective was attained using a bi-layer coating design composed of a nanothin hydrophobic underlayer with a toroidal, quaternary amine-bearing polymer microspot deposited on top. The coating methods were designed to enable the bulk production of analysis-ready filaments with a long shelf life. Standard and dimpled filaments were evaluated, as it was hypothesized that sample deposition into the concave well of the dimpled rhenium filament would promote ion formation and aid in direct loading by pipette.

2. Experimental section

2.1. Chemicals and materials

The following materials were used as received from Sigma-Aldrich: chloroform (Reagent Plus® ≥ 99.8% with 0.5–1.0% ethanol as stabilizer, CAS# 67-66-3); 1,4-diazabicyclo[2.2.2]octane (DABCO) (Reagent Plus® ≥ 99%, CAS# 280-57-9); hydrogen peroxide solution containing inhibitor (30 wt% in water, CAS# 7722-84-1); poly(vinylbenzyl chloride) (PVBC), (60/40 mixture of 3- and 4- isomers CAS# 121961-20-4); and sulfuric acid (95–98%, ACS reagent grade, CAS# 7664-93-9).

Hydrochloric acid (Optima™ grade for ultra-trace elemental analysis, CAS# 7647-01-0, 7732-18-5), methanol (Optima™ LC/MS grade, CAS# 67-56-1), nitric acid (Optima™ grade for ultra-trace elemental analysis, CAS# 7697-37-2, 7732-18-5) and triethylamine (TEA, 99%, reagent grade, CAS# 121-44-8) were used as received from Fisher Scientific.

Silicon substrates were acquired from Nova Electronic Materials as 4″ N/Ph < 100 > 1–10 Ω-cm 500–550 μm thick SSP prime grade Si wafers diced to 1 cm × 3 cm pieces. Anion-exchange resin beads were obtained from Bio-Rad (AG® 1-X2 Anion-exchange Resin, analytical grade, 50–100 mesh, chloride form). Collodion solution (flexible, CAS# for solution constituents: 60-29-7, 9004-70-0, 8001-79-4, 76-22-2, 64-17-5) was acquired from J.T. Baker. Rhenium ribbons (0.76 mm W × 0.03 mm H) and wafers (1 cm × 3 cm × 0.1 cm) were made of zone-refined rhenium (minimum of 4-pass zone refined; 99.999% Re) from H. Cross Company.

Pu solutions for TIMS measurements were prepared from a dilution of a primary standard containing New Brunswick Laboratory (NBL) certified reference material (CRM) 128 with a certified $^{239}Pu/^{242}Pu$ atom ratio of 0.99937 ± 0.00026 (determined October 1, 1984) at Savannah River National Laboratory (SRNL). Based on the half-lives of ^{239}Pu and ^{242}Pu, the approximated $^{239}Pu/^{242}Pu$ ratio would be 0.9985 on October 1, 2017. The decay corrected $^{239}Pu/^{242}Pu$ ratio (October 1, 2017) was used for calculating the deviation of measured ratios from

the certified value.

DI water with a resistance of 18.2 MΩ was prepared from distilled water that was passed through a Milli-Q water purification system (EMD-Millipore).

2.2. Construction and degassing of rhenium filament assemblies, resin bead loading, and TIMS instrument methodology

A consistent instrument methodology was used for all TIMS analyses (bead loading and thin film loading) operating an Isoprobe-T developed by IsotopX (Manchester, UK) and configured for nuclear applications. The construction and degassing of rhenium filament assemblies, bead loading, and TIMS instrument methodology used in this study are described in detail elsewhere [30,31]. A consistent warm-up routine was used for all analyses. Filament current was ramped at a rate of 0.2 A / min up to 3 A with two 5 min hold times at 1 and 2 A. Filament current was then increased manually in 0.05 A increments until an ion current of greater than 100 counts per second was detected at the 242 mass channel. The ion lenses were tuned manually to maximize the ion current. Ion production generally was witnessed at 3.2 A of filament current. Source and analyzer pressures were typically $5E^{-8}$ and $3E^{-9}$ Torr.

2.3. Silicon substrate preparation for polymer coating, atomic force microscopy, and ellipsometry

Methods for silicon substrate preparation and film characterization used in the study are described in detail elsewhere [32,33].

2.4. Polymer film formation: hydrophobic base layer

After degassing (in the case of rhenium filaments) or piranha washing (in the case of silicon wafers), substrates were dip-coated from solutions of PVBC in chloroform. (Safety note: Piranha solution is a mixture of sulfuric acid and hydrogen peroxide that reacts violently with organics. Special precautions should be followed for its safe use.) The film thickness produced by dip-coating depends on solution properties such as density, polymer concentration, and withdrawal rate [34]. To produce a film with a thickness of approximately 120 nm, the substrate was withdrawn from a 2 wt% PVBC solution at a withdrawal rate of 340 mm/min using a Qualtecs Product Industry QPI-128 dip coater. Immediately before dip-coating, DABCO was spiked into the solution to serve as a cross-linker. The molar amount of DABCO added was limited by stoichiometry based on a 1:2 reaction of DABCO to chloride sites along the PVBC chains. A ratio of 18.4 mg DABCO:1 g PVBC was used to prepare films with approximately 5% cross-linking. After dip-coating, filaments were placed in an 80 °C oven for 24 h to accelerate cross-linking of the films. Film thicknesses were determined with multi-angle ellipsometry. Fig. 1 shows a graphical representation of the dip-coating process and the chemicals involved.

2.5. Polymer preparation for toroidal polymer spots

A 10 wt% solution of PVBC in chloroform was prepared and 0.33 g TEA g^{-1} PVBC was added while stirring the solution magnetically. This solution was stirred continuously for approximately 48 h until a viscous TEA-quaternized PVBC polymer-rich phase formed. The chloroform was decanted from the polymer-rich liquid phase and discarded. The polymer-rich liquid phase was dried under vacuum (~ 16 kPa absolute pressure) for 48 h, ground with a glass stir rod (inside the scintillation vial used to perform the quaternization reaction), and placed under vacuum for an additional 24 h. The quaternization reaction between PVBC and TEA produces a water-soluble TEA-quaternized PVBC product.

2.6. Toroidal polymer spot formation using the "needle method"

Solutions from 0.5 to 10 wt% TEA-quaternized PVBC in deionized water were prepared alongside solutions of DABCO (0.275 g DABCO g^{-1} quaternized PVBC) in DI water. The TEA-quaternized PVBC and DABCO solutions were mixed for approximately 1 min immediately prior to spotting. Small spots were formed on PVBC-DABCO coated filaments and silicon wafers by the "needle method" (illustrated graphically in Fig. 2), which deposited a small droplet of the solution onto the PVBC-DABCO films. Based on the dimensions of deposited polymer spots (determined by 3-dimensional scanning electron microscopy and atomic force microscopy), droplets formed by the needle method are approximately 5–50 nL in volume. Spotted substrates were dried for 20 min at room temperature before being placed into an 80 °C oven for 24 h to accelerate cross-linking both within the deposited polymer spot and between the polymer spot and chlorobenzyl groups of the PVBC-DABCO film. Spot thickness was varied by changing the concentration of polymer in the spotting solution, and spot diameter was varied by changing the droplet volume.

2.7. 3-dimensional scanning electron microscopy (3D-SEM)

3D-SEM imaging was performed on a Hitachi S3400 variable pressure SEM at a pressure of 30 Pa. Variable pressure 3D-SEM was used to create 3D profiles of toroidal polymer spots. The following instrument

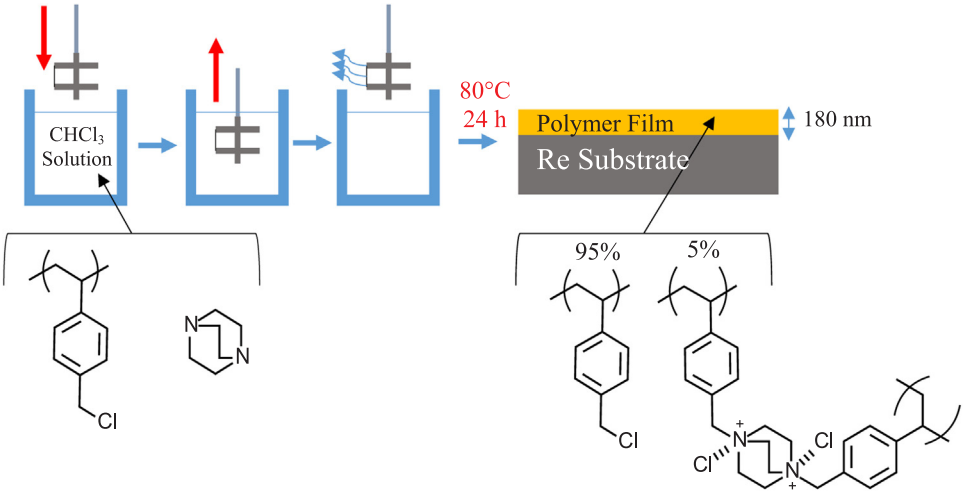

Fig. 1. Rhenium filament dip-coating procedure and film chemistry. (Left) Dip-coating was utilized to form the hydrophobic base polymer layer. PVBC and DABCO were dissolved in chloroform to prepare the dip-coating solution. The entire filament assembly was submerged and withdrawn from the dip-coating solution at a controlled rate. After solvent drying, the coated filaments were placed in an 80 °C oven for 24 h to accelerate reaction between the cross-linker (DABCO) and the polymer (PVBC). The cross-linked PVBC-DABCO films are hydrophobic and resist dissolution in both aqueous and organic solvents.

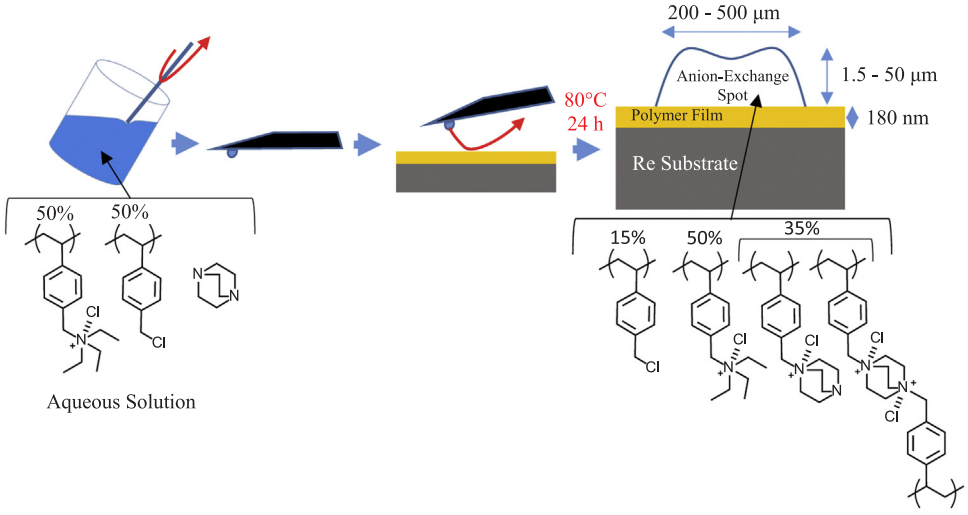

Fig. 2. "Needle method" developed to cast small polymer spots onto polymer-coated rhenium filaments. A steel needle was submerged into an aqueous solution of TEA-quaternized PVBC (approximately 50% conversion) and DABCO to deposit nanoliter droplets on the outside of the needle. The droplets were transferred to the surface of the coated filament by sweeping the needle across it. The sample was heated in an 80 °C oven for 24 h to accelerate cross-linking between DABCO-quaternized PVBC groups within the droplet and the underlying PVBC film, forming an insoluble hydrophilic island of anion-exchange polymer. The final polymer spots are approximately 200–500 µm wide and 1.5–50 µm thick based on the size of the droplet and concentration of polymer in the spotting solution.

settings were used for 3D imaging: 10 mm working distance, 15 kV acceleration voltage, 50 µA of probe current, backscatter mode, and a magnification of 100 ×. Silicon wafers that had been dip-coated and deposited with toroidal polymer spots were attached to SEM grids with carbon tape. 3D profiles were created using 3-D Image Viewer version 1.01 by combining images from four opposing backscatter detectors and calculating dimensions based on shading.

2.8. Sorption of Pu onto thin-film coated filaments

Thin-film coated filaments were direct loaded with 10 pg of NBL CRM 128 from either a 9 M HCl or 8 M HNO_3 matrix (5 µL deposited volume) onto the hydrophilic, spotted region of the film and dried using a heat lamp. Loading from an 8 M HNO_3 matrix was found to result in degradation of the rhenium substrate; therefore, 9 M HCl was used for the majority of these trials. After direct loading and drying under a heat lamp, filament assemblies were placed in the TIMS sample turret and analyzed.

3. Results and discussion

3.1. Thin film design and production

The thin-film design comprises two parts: 1) a hydrophobic underlayer (or base layer) composed of lightly cross-linked PVBC covering the entire filament surface, and 2) a small spot of TEA-quaternized and cross-linked PVBC positioned at the center of the filament, illustrated in Fig. 2. A polymer thin-film architecture was proposed for this work as it was hypothesized that migration and complexation of Pu into thin films would occur more rapidly than in the case of a bead, facilitating direct loading of the coated filament. Pu uptake studies were conducted with thin film chemistries utilized in this study, and maximum uptake was found to occur within 15 min of contact with Pu bearing solutions (with an anion-exchange capacity of $1.25 \times 10^{-4} \pm 1.07 \times 10^{-5}$ eq g^{-1} polymer) [32]. Additionally, it was hypothesized that by utilizing an extractant thin film, which places the Pu sample in close proximity to the ionization surface, higher ionization efficiencies would be attainable than in the case of bead loading due to increased transport and interaction with the ionization surface. In work by Smith et al. [22], it was shown that a graphitic, actinide bearing residue remains on filaments after heating beads, indicating that incomplete dissolution of the anion-exchange material into rhenium filaments occurs in the case of bead loading. Carbon is understood to be soluble in rhenium at elevated temperatures [19]. It was hypothesized within our group that more complete dissolution of anion-exchange material, and thus sample transport to the ionization surface, could be achieved with a thin film design through optimization of film thickness. It was also theorized that sample loss could be reduced by a thin-film design for similar reasons. Up to 25% sample loss has been reported when employing the bead loading method as a result of bead detachment during analysis [7]. In this study, we experienced no sample losses when analyzing thin film-coated filaments direct loaded from HCl (65 samples), in contrast to an approximate 15% loss rate with the bead loading method when using V-shaped filaments. We submit this is the result of greater contact area between the anion-exchange material and the surface in the case of the thin film design. Additionally, the thin film-coated filament design allows for direct loading by pipette instead of manual manipulation of small resin beads, a process that is tedious and susceptible to losses.

One reason for selecting an ion-exchange polymer is that Delmore [13,16] hypothesized, after work on the micro ion source program at Idaho National Laboratory, that the sample species must react chemically with carbon additives to effectively be converted to the carbide form. A quaternary amine-bearing polymer was selected for Pu loading due to a history of use in radiochemistry [35] and because the bead loading methodology uses Q-type resin beads [24]. PVBC is commercially available and offers a convenient platform to produce quaternary amine sites from a variety of alkyl-amine reagents. TEA was selected as the amination reagent due to its ease of use. Unlike trimethylamine, TEA is in a liquid state at room temperature. DABCO, a diamine, was used as a cross-linking agent to prevent dissolution of the TEA-quaternized PVBC spots when exposed to aqueous solutions and to affix spots chemically to the PVBC underlayer. Quaternary amine sites are produced in the reaction between DABCO and PVBC; therefore, it was theorized that high levels of cross-linking could be achieved without much sacrifice to ion-exchange capacity or hydrophilicity of the spots.

A thin underlayer of non-quaternized PVBC was first applied to the filaments by dip-coating and serves multiple purposes. 1) This layer provides chlorobenzyl groups for TEA-quaternized PVBC spots to attach via DABCO cross-links, preventing detachment of spots when they are swollen in the aqueous load solution. 2) The underlayer is hydrophobic, which aids in sample loading by driving aqueous load solutions towards the hydrophilic TEA-quaternized PVBC spot in the center of the filaments. We refer to this design as the "hydrophilic island". The aqueous Pu sample adheres to the hydrophilic spot when direct loaded and dries down onto the spot, leading to concentration of the sample in a geometrically small area. 3) The hydrophobic underlayer slows the aging of rhenium filaments under atmospheric conditions, extending the shelf life of degassed rhenium filaments [30,36]. We showed in a previous publication that humidity plays a significant role in the oxidation of rhenium filaments under atmospheric conditions and that filament oxidation reduces the sensitivity and reproducibility of TIMS measurements [30]. The hydrophobic film passivates rhenium filaments

against these detrimental effects for months. A reasonable filament shelf life is necessary for the viability of bulk filament preparation schemes proposed in this work. Dip-coating was selected as the production method for the PVBC underlayer due to its simplicity, scalability, and applicability to complex substrate geometries.

The anion-exchange region of the thin film design is limited to small spot of TEA-quaternized PVBC at the center of the filament. This geometry was developed to maintain a geometrically small ion pseudo-point source, similar in size to that of beads used in the resin bead method. Small spots were formed by placing a droplet of solution containing the TEA-quaternized PVBC and DABCO cross-linker in water onto the center of a PVBC-coated filament. Water was used as the solvent for deposition of spots because the applied droplets "bead up" on the hydrophobic underlayer and remain small. Spotting was performed by hand for the samples presented in this study; however, the feasibility of using a piezoelectric nano-dropper to form anion-exchange polymer spots was investigated at the end of the project, and the resulting spot geometry is consistent with manually deposited spots. The use of traditional pipettes to deposit spots was not possible due to the small droplet volumes needed (5–50 nL for sub-500 µm diameter droplets). In the case of bulk filament production, we envision the use of equipment such as nano-dropper arrays to automate the spotting process for a large number of filaments.

3.2. Manipulation of anion-exchange spot dimensions

Variable pressure 3D SEM and AFM were used to image and obtain height profiles of spots. Fig. 3 and Fig. S-1 show that the deposited spots are toroidal in shape with a thick outer rim. This shape was consistent with thinner spots imaged with AFM (Fig. S-2) and is the product of a phenomena referred to as the "coffee ring effect", where capillary forces in the drying droplet drive polymer to the edge of the spot [37]. In this paper, we define the spot "thickness" as the maximum height of the toroidal ring. Spot thickness was varied by changing the concentration of polymer in the aqueous deposition solution from 0.5 to 10 wt% and maintaining the deposited droplet volume. Fig. 4 shows the relationship between polymer concentration and spot thickness acquired with AFM. The maximum height measureable by the AFM used in this study is 7 µm; therefore, the relationship shown in Fig. 4 was used to estimate the thickness of spots with intermediate thicknesses (7–30 µm) that were difficult to profile by 3D-SEM due to low levels of shading.

Spot diameter is a function of the deposited droplet volume. It was determined through optical microscopy and SEM that spot diameters ranged from approximately 200 to 500 µm when using the needle method. Smaller spots were used in the TIMS studies presented; however, initial measurements determined that variability in spot diameter did not appear to impact performance significantly in terms of measurement sensitivity or reproducibility. Spot thickness on the other hand did impact analytical performance and is described in the following section.

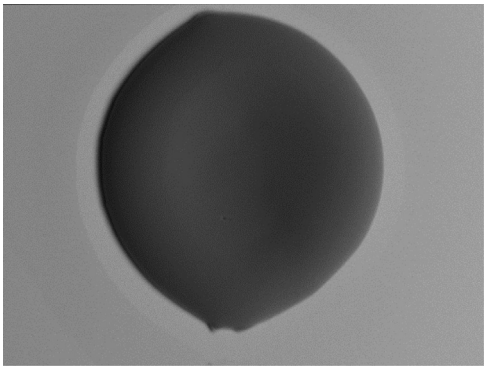

Fig. 3. 3D SEM image of ion-exchange polymer spot.

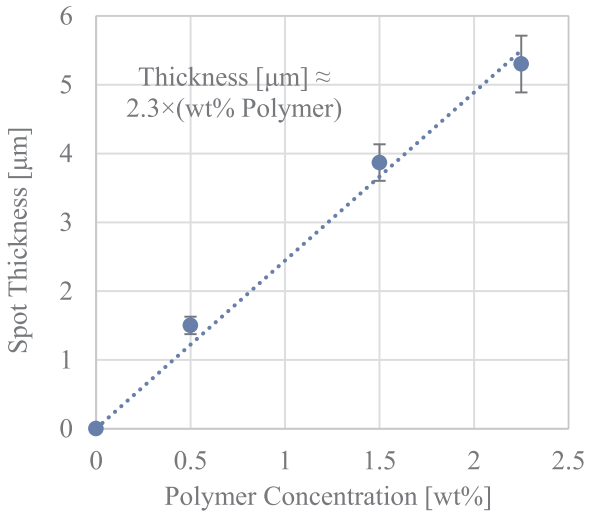

Fig. 4. Relationship between polymer concentration in spotting solution and resulting polymer spot thickness. Thicknesses were determined by AFM measurements, and the fitted relationship was used to estimate spot thickness for solutions with concentrations greater than 2.25 wt% polymer.

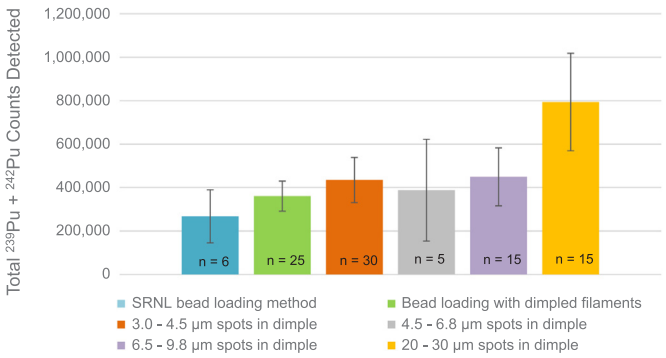

Fig. 5. Comparison of the average ion counts for toroidal spots in dimpled filaments, the established SRNL bead loading method (with V-Shaped filaments), and the bead loading method with dimpled filaments, using a constant 10 pg load of Pu. All spotted filaments were direct loaded from a 9 M HCl matrix. Beads were loaded with Pu from 8 M HNO_3. Error bars represent 95% confidence intervals.

3.3. Thermal ionization mass spectrometry

Thermal ionization mass spectrometry was performed at SRNL and details of the instrument methodology are described elsewhere [31]. Fig. 5 and Table S-1 compares sample utilization from various loading strategies given a 10 pg load of NBL CRM 128. Hydrochloric acid was used for direct loading of thin films to prevent corrosion of the filament surface leading to polymer spot detachment. This phenomenon is highlighted in Table S-2 where thin spots (1.0–1.5 µm) were direct loaded from both 8 M HNO_3 and 9 M HCl solutions. Acid stability studies within our group have shown that 8 M HNO_3 solutions aggressively corrode rhenium surfaces, even when these surfaces are coated with a hydrophobic PVBC-DABCO film (Fig. S-3). An HCl direct loading matrix was used for all subsequent measurements using the toroidal spot design.

Sample utilization was found to depend strongly on the thickness of the anion-exchange spots deposited onto filaments. In our original design, anion-exchange spots were approximately 200 nm thick. These filaments performed poorly when compared to those loaded with resin beads, producing a comparable number of counts to samples loaded directly on carburized filaments (data not shown). Increasing the thickness of anion-exchange spots to 1.0–1.5 µm improved sample

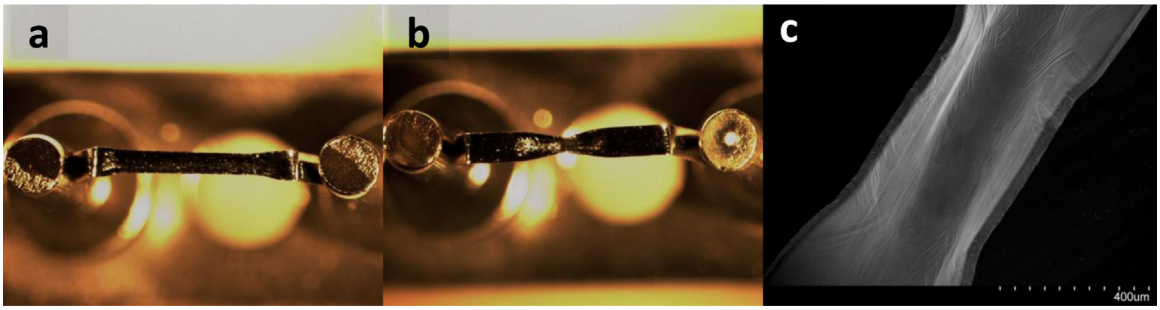

Fig. 6. a) Traditional "boat" or V-shaped filament design. b) Dimpled filament design presented in this work. c) SEM image of the crimped region of a dimpled rhenium filament.

utilization by approximately 400%, but utilization remained low compared to the bead method, and the filaments only produced ions for approximately 1 h. To increase the duration of ion production, the thickness of anion-exchange spots was increased to 3.0–4.5 μm by increasing polymer concentration from 0.5 to 1.5 wt% in the spotting solution and maintaining the volume of the deposited droplet. These thicker spots were found to produce ions for approximately 3 h on flat filaments, a proportional increase in duration of ion production. However, the total counts produced was ~10 times more than the 1.0–1.5 μm spots and reached levels of sample utilization comparable to the resin bead method.

The efficacy of dimpled filaments was explored to further increase sample utilization. Fig. 6 compares the dimpled filament design to that of the "boat" or V-shaped filament design and shows an SEM image of the dimpled region of a rhenium filament. Ion-exchange polymer spots with a thickness of 3.0–4.5 μm were formed on dimpled filaments, resulting in a 25% increase in the duration of ion production (increased from 3 to 3.75 h) and a 43% increase in total counts compared to similar spots cast on flat filaments. We submit that the increased sample utilization experienced with dimpled filaments is the result of a concave filament structure. Similarly to cavity sources, when the sample is loaded into the well of a concave dimple, neutral gas atoms have opportunity to interact with the ionization surface after volatilization from the load region, resulting in higher ionization efficiencies. Dimpled filaments also aid in direct sample loading as they allow the sample to be placed in a cup-like substrate. Combined with the hydrophilic island created by the bi-layer film design, it is relatively simple to consistently deposit the sample in small region in the geometric center of the filament. Due to the benefits of dimpled filaments, they were used for all subsequent thin film-loading measurements in this study.

Although an inadequate number of trials have been performed to state with any significant statistical confidence that dimpled filaments improve sensitivity using bead loading, based on the trial runs for this study and experience at SRNL, the use of dimpled filaments (over that of V-shaped filaments) appears to increase measurement sensitivity by about 30%. More importantly, no sample losses have been experienced when beads are loaded onto dimpled filaments, compared to the 15–20% sample loss routinely experienced when loading beads onto V-shaped filaments. In-instrument sample loss is a notorious problem when employing the bead loading method [7], so overcoming it represents a major accomplishment. We submit that the reduction in sample loss when using dimpled filaments is the result of greater contact between beads and the ionization surface and reduced bead migration during heating. Additionally, the use of dimpled filaments aids in transferring and positioning beads in the geometric center of filaments.

To further improve the ionization efficiency provided by the thin film method, anion-exchange spot thickness was increased by depositing droplets of 2.25, 3.25, and 10 wt% polymer solutions, producing spot thicknesses of 4.5–6.8 μm, 6.5–9.8 μm, and 20–30 μm. Toroidal spots with a thickness of 20–30 μm provided the highest sample utilization (Fig. 5), surpassing the sample utilization of the standard SRNL bead loading method by 175%. Additionally, no filament failures were experienced over the course of analyzing 65 filaments with toroidal spots. Fig. 7 compares uncorrected isotopic ratios obtained from thin film-coated filaments and the established bead-loading method. These finding are in good agreement with the certified $^{239}Pu/^{242}Pu$ ratio for NBL CRM 128. The reported sample utilization is low (< 0.1% based on the ^{239}Pu and ^{242}Pu duty cycles); however, this is due to the instrument used for these analyses. The reported ion counts are intended for comparative analysis rather than a representation of absolute detection limits based on the sample loading method. The IsotopX TIMS used in this study is utilized for research purposes at SRNL; whereas, a custom-built 3-stage TIMS is reserved for environmental sample analyses and routinely reaches ~1% sample utilization with the SRNL bead loading methodology.

We submit that the improved sample utilization achieved with the toroidal spot loading technique, compared to bead loading, is due to increased sample transport and interaction with the ionization surface. Additionally, we hypothesize that increasing the thickness of toroidal spots improved sample utilization by promoting the formation of Pu-carbides through higher C/Pu ratios. It is now evident that there must be a balance between limiting the amount of carbon material (i.e., spot thickness should be smaller than the diameter of a standard resin bead) so that sample transport to the ionization surface can occur and providing enough carbon to promote the formation and persistence of Pu-carbides on the filament surface. Therefore, an optimum spot thickness exists that balances these two processes. Unfortunately, funding for this

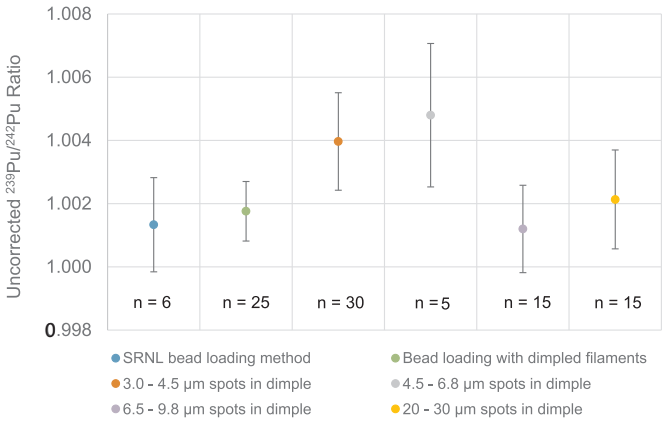

Fig. 7. Comparison of isotope ratios for spots dimpled filaments, the SRNL bead method (with V-shaped filaments), and the bead loading method with dimpled filaments, using a constant 10 pg load of Pu. Error bars represent 95% confidence intervals. The decay corrected (Oct. 1, 2017) $^{239}Pu/^{242}Pu$ ratio for CRM 128 is 0.9985.

project ended before the design could be optimized. We do not believe that the benefits of increasing spot thickness are related to Pu capacity of the spots, as the number of ion-exchange sites on even the thinnest spots (1–3 μm in thickness, 200 μm in diameter) is two to three orders of magnitude higher than the number of moles of Pu in the loading solution (with 10 pg of Pu). The level of improvement (over the bead loading method) in terms of sample utilization when fiber loading (180%) [31] or thin film loading (175%) is greater than that reported for other methods of TIMS sample loading currently under development, such as the PIE design (154%) [38]. This finding illuminates the importance of anion-exchange material design in the development of improved sample loading techniques for TIMS.

4. Conclusions

A sample loading strategy based on polymer thin-film coatings was developed that surpasses sample utilization afforded by the bead loading method. The coating simplifies sample loading by enabling direct loading in the geometric center of filaments. Coated filaments also eliminate sample loss, a problem often encountered when employing the bead loading strategy. Although preparation of coated filaments requires a two-step process, the thin film design allows for automated bulk production of pre-coated, analysis-ready filaments with long shelf lives. This capability is a major advancement over the bead loading method and other methods that rely on the material being submerged in the sample bearing solution before being individually manipulated and affixed to the filament. A quaternary amine-bearing polymer was used in this study; however, the general methodology of polymer thin-film and spot production can be extended to other polymer and ligand systems, and automated using well-established coating and droplet dispensing technologies.

Acknowledgements

This work was supported by the National Nuclear Security Administration NA-221 Office of Proliferation Detection [Award No. DE-NA0001735]. The authors thank Taghi Darroudi and other members of the Clemson University Electron Microscopy Laboratory for their assistance with 3D SEM analyses.

Notes

The authors declare no competing financial interests.

Supporting information

Comparison and statistics of sample utilization among explored methods; effect of acid matrix on performance; 3-D SEM cross-section of polymer; AFM profiles of polymer; nitric acid corrosion of rhenium.

Appendix A. Supporting information

Supplementary data associated with this article can be found in the online version at doi:10.1016/j.talanta.2018.07.048.

References

[1] S.K. Aggarwal, Thermal ionisation mass spectrometry (TIMS) in nuclear science and technology – a review, Anal. Methods 8 (5) (2016) 942–957.
[2] L.N. Elliot, A.G. Bickel, H.S. Linauskas, M.L. Paterson, Determination of femtogram quantities of 239Pu and 240Pu in bioassay samples by thermal ionization mass spectrometry, J. Radioanal. Nucl. Chem. 267 (3) (2006) 637–650.
[3] C.-G. Lee, D. Suzuki, F. Esaka, M. Magara, K. Song, Ultra-trace analysis of plutonium by thermal ionization mass spectrometry with a continuous heating technique without chemical separation, Talanta 141 (2015) 92–96.
[4] S. Boulyga, S. Konegger-Kappel, S. Richter, L. Sangely, Mass spectrometric analysis for nuclear safeguards, J. Anal. At. Spectrom. 30 (7) (2015) 1469–1489.
[5] D. Suzuki, F. Esaka, Y. Miyamoto, M. Magara, Direct isotope ratio analysis of individual uranium–plutonium mixed particles with various U/Pu ratios by thermal ionization mass spectrometry, Appl. Radiat. Isot. 96 (2015) 52–56.
[6] Y. Shibahara, T. Kubota, T. Fujii, S. Fukutani, K. Takamiya, M. Konno, S. Mizuno, H. Yamana, Determination of isotopic ratios of plutonium and uranium in soil samples by thermal ionization mass spectrometry, J. Radioanal. Nucl. Chem. 307 (3) (2016) 2281–2287.
[7] M.G. Watrous, J.E. Delmore, M.L. Stone, Porous ion emitters—a new type of thermal ion emitter, Int. J. Mass Spectrom. 296 (1–3) (2010) 21–24.
[8] H. Kurosaki, D. Chang, K.G.W. Inn, In search of higher sensitivity: Pu isotopic analysis, J. Radioanal. Nucl. Chem. 269 (2) (2006) 279–281.
[9] S. Bürger, L.R. Riciputi, D.A. Bostick, S. Turgeon, E.H. McBay, M. Lavelle, Isotope ratio analysis of actinides, fission products, and geolocators by high-efficiency multi-collector thermal ionization mass spectrometry, Int. J. Mass Spectrom. 286 (2–3) (2009) 70–82.
[10] S. Bürger, S.D. Balsley, S. Baumann, J. Berger, S.F. Boulyga, J.A. Cunningham, S. Kappel, A. Koepf, J. Poths, Uranium and plutonium analysis of nuclear material samples by multi-collector thermal ionisation mass spectrometry: quality control, measurement uncertainty, and metrological traceability, Int. J. Mass Spectrom. 311 (2012) 40–50.
[11] M.H. Studier, E.N. Sloth, L.P. Moore, The chemistry of uranium in surface ionization sources, J. Phys. Chem. 66 (1) (1962) 133–134.
[12] J.M. Kelley, D.M. Robertson, Plutonium ion emission from carburized rhenium mass spectrometer filaments, Anal. Chem. 57 (1) (1985) 124–130.
[13] M.G. Watrous, J.E. Delmore, Metal dicarbides as intermediate species in thermal ion formation mechanisms, Int. J. Mass Spectrom. 286 (1) (2009) 7–10.
[14] M.J. Dresser, The Saha-Langmuir equation and its application, J. Appl. Phys. 39 (1) (1968) 338–339.
[15] H. Kawano, Effective work functions for ionic and electronic emissions from mono- and polycrystalline surfaces, Prog. Surf. Sci. 83 (1–2) (2008) 1–165.
[16] J.E. Delmore, Micro Ion Source Program NA22 Plutonium Detection Portfolio Final Report, Idaho National Laboratory (United States). Funding organisation: DOE-NA (United States), 2010.
[17] R. Jakopič, S. Richter, H. Kühn, L. Benedik, B. Pihlar, Y. Aregbe, Isotope ratio measurements of pg-size plutonium samples using TIMS in combination with “multiple ion counting” and filament carburization, Int. J. Mass Spectrom. 279 (2–3) (2009) 87–92.
[18] D.H. Smith, J.A. Carter, A simple method to enhance thermal emission of metal ions, Int. J. Mass Spectrom. Ion. Phys. 40 (2) (1981) 211–215.
[19] P.G. Pallmer, R.L. Gordon, M.J. Dresser, The work function of carburized rhenium, J. Appl. Phys. 51 (7) (1980) 3776–3779.
[20] R. Jakopic, S. Richter, H. Kuhn, Y. Aregbe, Determination of 240Pu/239Pu, 241Pu/239Pu and 242Pu/239Pu isotope ratios in environmental reference materials and samples from Chernobyl by thermal ionization mass spectrometry (TIMS) and filament carburization, J. Anal. At. Spectrom. 25 (6) (2010) 815–821.
[21] D.M. Wayne, W. Hang, D.K. McDaniel, R.E. Fields, E. Rios, V. Majidi, The thermal ionization cavity (TIC) source: elucidation of possible mechanisms for enhanced ionization efficiency, Int. J. Mass Spectrom. 216 (1) (2002) 41–57.
[22] D.H. Smith, W.H. Christie, R.E. Eby, The resin bead as a thermal ion source: a sims study, Int. J. Mass Spectrom. Ion. Phys. 36 (3) (1980) 301–316.
[23] M. Kraiem, K. Mayer, T. Gouder, A. Seibert, T. Wiss, H. Thiele, J.P. Hiernaut, Experimental investigation of the ionization mechanisms of uranium in thermal ionization mass spectrometry in the presence of carbon, Int. J. Mass Spectrom. 289 (2–3) (2010) 108–118.
[24] J.D. Fassett, W.R. Kelly, Interlaboratory isotopic ratio measurement of nanogram quantities of uranium and plutonium on resin beads by thermal ionization mass spectrometry, Anal. Chem. 56 (3) (1984) 550–556.
[25] J. Navratil, L. Martella, Comparison of anion exchange resins for recovering plutonium from nitric acid waste, Nucl. Technol. 46 (1) (1979) 105–109.
[26] A.R. King, D. Knight, A. Fairhead, Analysis of uranium and plutonium following adsorption on actinide resin, J. Radioanal. Nucl. Chem. 304 (1) (2015) 163–169.
[27] S. Bürger, L.R. Riciputi, S. Turgeon, D. Bostick, E. McBay, M. Lavelle, A high efficiency cavity ion source using TIMS for nuclear forensic analysis, J. Alloy. Compd. 444–445 (2007) 660–662.
[28] L.A. Dietz, Ion optics for the V-type surface ionization filament used in mass spectrometry, Rev. Sci. Instrum. 30 (4) (1959) 235–241.
[29] S. Paul, A.K. Pandey, R.V. Shah, K.S. Bhushan, S.K. Aggarwal, Polymer based sorbent materials for thermal ionization mass spectrometric determination of uranium(vi) and plutonium(iv) ions, J. Anal. At. Spectrom. 31 (4) (2016) 985–993.
[30] J.M. Mannion, J.C.R. Shick, G.A. Fugate, M.S. Wellons, B.A. Powell, S.M. Husson, Rhenium filament oxidation: effect on TIMS performance and the roles of carburization and humidity, Talanta 168 (2017) 183–187.
[31] J.M. Mannion, C.R. Shick Jr, G.A. Fugate, B.A. Powell, S.M. Husson, Anion-exchange fibers for improved sample loading in ultra-trace analysis of plutonium by thermal ionization mass spectrometry, Anal. Chem. 89 (17) (2017) 8638–8642.
[32] W.D. Locklair, J.M. Mannion, S.M. Husson, B.A. Powell, Uptake of plutonium on a novel thin film for use in spectrometry, J. Radioanal. Nucl. Chem. 307 (3) (2016) 2333–2338.
[33] J.M. Mannion, W.D. Locklair, B.A. Powell, S.M. Husson, Alpha spectroscopy substrates based on thin polymer films, J. Radioanal. Nucl. Chem. 307 (3) (2016) 2339–2345.
[34] J. Zhou, J. Jin, A.T. Haldeman, E.H. Wagener, S.M. Husson, Formation and characterization of perfluorocyclobutyl polymer thin films, J. Appl. Polym. Sci. 129 (6) (2013) 3226–3236.
[35] J. Ryan, E. Wheelwright, The recovery, purification, and concentration of plutonium by anion exchange in nitric acid, General Electric Co. Hanford Atomic Products Operation, Richland, Wash, 1959.
[36] W.M.S. Mannion J.M, C.R. Shick, G.A. Fugate, B.A. Powell, S.M. Husson, Ambient aging of rhenium filaments used in thermal ionization mass spectrometry: growth of oxo-rhenium crystallites and anti-aging strategies, Heliyon 3 (1) (2017).
[37] P.J. Yunker, T. Still, M.A. Lohr, A. Yodh, Suppression of the coffee-ring effect by shape-dependent capillary interactions, Nature 476 (7360) (2011) 308–311.
[38] M.L. Baruzzini, H.L. Hall, M.G. Watrous, K.J. Spencer, F.E. Stanley, Enhanced ionization efficiency in TIMS analyses of plutonium and americium using porous ion emitters, Int. J. Mass Spectrom. 412 (2017) 8–13.